

Determinant-based Fast Greedy Sensor Selection Algorithm

Yuji Saito, Taku Nonomura, Keigo Yamada, Keisuke Asai

Tohoku University, Sendai, Miyagi 980-8579, Japan

Yasuo Sasaki, and Daisuke Tsubakino

Nagoya University, Nagoya, Aichi, 464-8603, Japan

Abstract—In this study, the sparse sensor placement problem for the least square estimation is considered. First, the objective function of the problem is redefined to be the maximization of determinant of the matrix appearing in pseudo inverse matrix operations, leading to the maximization of the corresponding confidence intervals. The procedure for the maximization of determinant of the corresponding matrix is proved to be the same as that of the previous QR method in the case of the number of sensors less than that of state variables. On the other hand, the authors have developed the new algorithm in the case of the number of sensors greater than that of state variables. Then, the unified formulation of both algorithms is derived, and the lower bound of the objective function given by this algorithm is shown using the monotone submodularity. In a new algorithm, optimal sensors are obtained by QR method until the number of sensors is equal to state variables and, after that, new sensors are calculated by a proposed determinant-based greedy method which is accelerated by both determinant formula and matrix inversion lemma. The effectiveness of this algorithm on data-sets related to global climate dataset is demonstrated by comparing with the results by the other algorithms. The calculation results

show that the calculation time of the proposed extended determinant-based greedy algorithm is smaller than that of other methods with almost the minimum level of estimation errors.

Index Terms—Data processing, sensor placement, greedy algorithm.

I. INTRODUCTION

Recently, reduced-order modeling for fluid analysis and flow control gather a lot of attentions. With regard to reduced-order modeling, proper orthogonal decomposition (POD)[1], [2] is one of the effective methods to decompose the high-dimension fluid data into several significant modes of flow fields. Here, POD is a data-driven method which gives us the most significant and relevant structure in the data, and it exactly corresponds to principal component analysis and Karhunen-Loeve (KL) decomposition, where the decomposed modes are orthogonal each other. The POD analysis for discrete data matrix can be carried out by applying the singular value decomposition, as is often the case in the engineering fields. Although there are several advanced data-driven methods, dynamic mode decomposition[3], [4], empirical mode decomposition, and others which include efforts by the present authors[5], [6], this research is

Assistant Professor, Department of Aerospace Engineering.

Associate Professor, Department of Aerospace Engineering, also
Presto, JST.

Graduate student, Department of Aerospace Engineering.

Professor, Department of Aerospace Engineering.

Graduate student, Department of Aerospace Engineering.

Lecturer, Department of Aerospace Engineering.

only based on POD which is the most basic data-driven method for reduced-order modeling.

If the data, such as flow fields, can be effectively expressed by a limited number of POD modes, the limited sensor placed at appropriate positions gives us the approximated full state information. This effective observation might be one of the keys for flow control and flow prediction. This idea has been adopted by Manohar et al.[7], and the sparse-sensor-placement algorithm has been developed and discussed. The idea here is expressed by the following equation:

$$\begin{aligned} \mathbf{y} &= \mathbf{H} \mathbf{U} \mathbf{x} \\ &= \mathbf{C} \mathbf{x}. \end{aligned} \quad (1)$$

Here, $\mathbf{y} \in \mathbb{R}^p$, $\mathbf{x} \in \mathbb{R}^r$, $\mathbf{H} \in \mathbb{R}^{p \times n}$ and $\mathbf{U} \in \mathbb{R}^{n \times r}$ are the observation vector, the POD mode amplitude, the sparse sensor location matrix, and spatial POD modes, respectively. In addition, p , n , and r are numbers of sensor location, degrees of freedom of the spatial POD modes, and the rank for truncated POD, respectively. The problem above is considered to be one of the sensor selection problems when the POD mode \mathbf{U} and strength \mathbf{x} are assumed to be a sensor-candidate matrix and the latent state variables, respectively. The graphical image of the equation above is shown in Fig. 1.

The optimal sensor placement is an important challenge in the design, prediction, estimation, and control of high-dimensional systems. High-dimensional states can often leverage a latent low-dimensional representation, and this inherent compressibility enables sparse sensing. For example, in the applications of aerospace engineering, such as launch vehicle and satellite, the optimal sensor placement is an important subject in performance prediction, control of the system, fault diagnostics and prognostics, etc. because of the limitation of the installation, limitation of cost, and limitation of downlink capacity transferring measurement data. Therefore, the

study on the optimal sensor placement is valuable in this field. Those sparse point sensors should be selected considering the POD modes. Although compressed sensing can recover a wider class of signals, the benefits of exploiting known patterns in data with optimized sensing is utilized, as similar to the previous study[7]. In this case, drastic reductions in the required number of sensors and improved reconstruction can be expected.

Thus far, this sensor selection problem has been solved by a convex approximation and a greedy algorithm, where the greedy algorithm was shown to be much faster than the convex approximation algorithms. Table I summarizes a computational complexity based on each calculation methods: the brute-force searching, the convex approximation method, and the greedy algorithm, respectively. The previous study [7] introduced that the greedy algorithm is based on QR-discrete-empirical-interpolation method [8], [9] when the number of the sensors is the same as that of state variables and its extension for the least square problem when the number of the sensor is greater than that of state variables. Both convex approximation and greedy algorithm work pretty well for the sensor selection problems. However, in the greedy algorithm, when the number of the sensor is greater than that of state variables, the theoretical background for calculation is not clear and has not been developed in the previous study. Therefore, the present paper introduces a new formulation and presents its monotone submodularity and performance. In a new algorithm, optimal sensors are obtained by QR method until the number of sensors is equal to state variables and, after that, new sensors are calculated by a proposed determinant-based greedy method which is accelerated by both determinant formula and matrix inversion lemma.

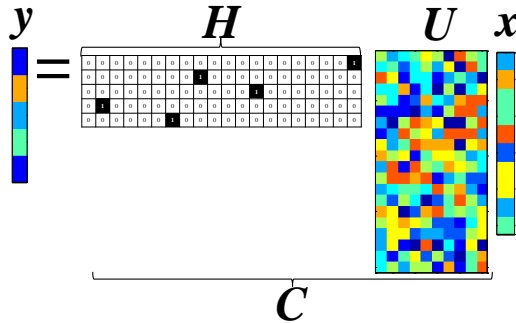


Fig. 1. Graphical image for sensor matrix \mathbf{H} on Eq.1

TABLE I
RUN TIME OF EACH METHOD FOR SELECTING SENSORS[7].

| Name | Run time |
|-----------------------------|-----------------------------------|
| Brute-force search | $\frac{n!}{(n-p)!p!} \sim O(n^p)$ |
| Convex approximation method | $O(n^3)$ per iteration. |
| Greedy method | $O(np^2)$ |

II. ALGORITHM

A. Previous Greedy Algorithm for Sensors

In the greedy algorithm based on QR decomposition for scalar measurement problem, i -th sensor is chosen where

$$i = \arg \max \|\mathbf{v}_i\|_2^2. \quad (2)$$

Here, we initialize $\mathbf{v}_i = [V_{i,1} \ V_{i,2} \ \dots \ V_{i,r}]$ and $\{V_{ij}\} = \mathbf{V} = \mathbf{U}$ and $\{V_{ij}\} = \mathbf{V} = \mathbf{U}\mathbf{U}^T$ for $p = r$ and $p > r$ sensor conditions, respectively, as did in the previous study[7]. Given i index, the \mathbf{V} matrix is pivoted and QR decomposed using newly selected \mathbf{v}_i . After that, the next sensor is chosen for remaining matrix. The algorithms for $p = r$ and $p > r$ sensors are QR-discrete-empirical-interpolation method (QDEIM) and optimized sparse sensor placement as an extension of QDEIM, respectively.

In case of $p = r$, the optimization is considered to conduct the maximization of determinant of the \mathbf{C}

matrix to stably solve \mathbf{x} vector. The selection of the sensor position is based on maximizing the norm of the corresponding row vector of the sensor-candidate matrix. On the other hand, the calculation algorithm for the condition $p > r$ has already been proposed in the previous study (which corresponds to the use of $\mathbf{V} = \mathbf{U}\mathbf{U}^T$ instead of $\mathbf{V} = \mathbf{U}$), but, the validity of the algorithm has not been explained and clarified well in the previous study. This equivalent Gram-Schmidt algorithm to the previous QR algorithm is shown in Alg.1.

Algorithm 1 Greedy algorithm for sparse sensor placement

Set sensor-candidate matrix \mathbf{U} .

Set number of sensors $p \geq r$.

if $p = r$ **then**

$\mathbf{V} = \mathbf{U}$

else if $p > r$ **then**

$\mathbf{V} = \mathbf{U}\mathbf{U}^T$

end if

for $k = 1, \dots, p$ **do**

$\mathbf{v}_i = [V_{i1} \ V_{i2} \ \dots \ V_{ir}]$

$i \leftarrow \arg \max_i \|\mathbf{v}_i\|_2^2$

$\mathbf{w}_k \leftarrow \mathbf{v}_i$

$\mathbf{V} \leftarrow \mathbf{V} - \mathbf{V}\mathbf{w}_k^T \mathbf{w}_k / \|\mathbf{w}_k\|_2^2$

$H_{k,i} = 1$

end for

B. Proposed Determinant-based Greedy Algorithm

Let \mathbf{C}_k denotes k th sensor-candidate matrix as follows:

$$\mathbf{C}_k = [\mathbf{u}_{i_1}^T \ \mathbf{u}_{i_2}^T \ \dots \ \mathbf{u}_{i_{k-1}}^T \ \mathbf{u}_{i_k}^T]^T, \quad (3)$$

where i_k and \mathbf{u}_{i_k} are an index of the k th selected sensor and the corresponding row vector of the sensor-candidate matrix. By extending this sensor-candidate matrix to the pseudo inverse matrix, the following algorithm can be derived straightforwardly. The sensor-selection problem

is defined as we know sensor locations of $(k-1)$ th sensor selected thus far. Equation 1 can be solved as $\mathbf{x} = \mathbf{C}^+ \mathbf{y}$ and divided into two cases:

$$\mathbf{x} = \begin{cases} \mathbf{C}^T (\mathbf{C}\mathbf{C}^T)^{-1} \mathbf{y}, & p \leq r, \\ (\mathbf{C}^T \mathbf{C})^{-1} \mathbf{C}^T \mathbf{y}, & p > r. \end{cases} \quad (4)$$

Here, \mathbf{C} is assumed to be a column-full-rank or row-full-rank matrix. Therefore, the optimization could also be divided into two cases: the maximization of determinant of $\mathbf{C}\mathbf{C}^T$ and $\mathbf{C}^T\mathbf{C}$ in the cases of $p \leq r$ and $p > r$, respectively. In the greedy algorithm, the sensors up to $k-1$ are already selected and it becomes the sensor selecting problem only k . The subject is expressed as Algorithm 2 summarizes. The problem in the case of $k \leq r$ has been conducted by Manohar et al. [10]. As explained before, their algorithm selects the sensor position based on maximizing the norm of the corresponding row vector of the sensor-candidate matrix \mathbf{U} applying the QR decomposition. Although they explained in [10] that the QR decomposition provides an approximate greedy solution for the maximization of the determinant of \mathbf{C} , to the best of our knowledge, they have yet to explain this mathematical background in detail. Therefore, the mathematical background for the maximization of determinant of $\mathbf{C}\mathbf{C}^T$ will be described in the next section. The problem in the case of $k > r$ has been conducted in previous studies [11] [12], and the proposing objective function in this study (the maximization of determinant of $\mathbf{C}^T\mathbf{C}$) corresponds to designing the experiment to minimize the volume of the resulting confidence ellipsoid[11].

In the case of $k \leq r$, the step-by-step maximization of the determinant of $\mathbf{C}_k \mathbf{C}_k^T$ is considered using the greedy method. This objective is the maximization of the determinant of the matrix appearing in pseudo inverse matrix operations, leading to the maximization of confidence intervals. It can be expanded as follows (see, e.g., [13]

Algorithm 2 Overview of Determinant-based greedy algorithm for sparse sensor placement

```

for  $k = 1, \dots, r, \dots, p$  do
    if  $k = 1$  then
         $i_k = \arg \max_i \mathbf{u}_i \mathbf{u}_i^T$ 
    else if  $k \leq r$  then
         $i_k = \arg \max_i \det(\mathbf{C}_k \mathbf{C}_k^T)$ 
         $= \arg \max_i \det \left( \begin{bmatrix} \mathbf{C}_{k-1} \\ \mathbf{u}_i \end{bmatrix} \left[ \begin{array}{cc} \mathbf{C}_{k-1}^T & \mathbf{u}_i^T \end{array} \right] \right)$ 
    else
         $i_k = \arg \max_i \det(\mathbf{C}_k^T \mathbf{C}_k)$ 
         $= \arg \max_i \det \left( \begin{bmatrix} \mathbf{C}_{k-1}^T & \mathbf{u}_i^T \end{bmatrix} \left[ \begin{array}{c} \mathbf{C}_{k-1} \\ \mathbf{u}_i \end{array} \right] \right)$ 
    end if
    Set sensor-candidate matrix
     $\mathbf{C}_k = [\mathbf{u}_{i_1}^T \mathbf{u}_{i_2}^T \dots \mathbf{u}_{i_{k-1}}^T \mathbf{u}_{i_k}^T]^T$ 
end for

```

for detailed derivation):

$$\begin{aligned}
\det(\mathbf{C}_k \mathbf{C}_k^T) &= \det \left(\begin{bmatrix} \mathbf{C}_{k-1} & \mathbf{u}_i \end{bmatrix} \left[\begin{array}{c} \mathbf{C}_{k-1}^T \\ \mathbf{u}_i^T \end{array} \right] \right) \\
&= \det(\mathbf{C}_{k-1} \mathbf{C}_{k-1}^T + \mathbf{u}_i \mathbf{u}_i^T) \\
&= (\det \mathbf{C}_{k-1} \mathbf{C}_{k-1}^T) \\
&\quad \left(\mathbf{u}_i \mathbf{u}_i^T - \mathbf{u}_i \mathbf{C}_{k-1}^T (\mathbf{C}_{k-1} \mathbf{C}_{k-1}^T)^{-1} \mathbf{C}_{k-1} \mathbf{u}_i^T \right) \\
&= (\det \mathbf{C}_{k-1} \mathbf{C}_{k-1}^T) \\
&\quad \mathbf{u}_i \left(\mathbf{I} - \mathbf{C}_{k-1}^T (\mathbf{C}_{k-1} \mathbf{C}_{k-1}^T)^{-1} \mathbf{C}_{k-1} \right) \mathbf{u}_i^T, \quad (5)
\end{aligned}$$

and, therefore,

$$\begin{aligned}
&\arg \max \det(\mathbf{C}_k \mathbf{C}_k^T) \\
&= \arg \max \mathbf{u}_i \left(\mathbf{I} - \mathbf{C}_{k-1}^T (\mathbf{C}_{k-1} \mathbf{C}_{k-1}^T)^{-1} \mathbf{C}_{k-1} \right) \mathbf{u}_i^T. \quad (6)
\end{aligned}$$

In the k th step of sensor selection of the previous QR (or Gram-Schmidt) method and the present method, the following equality is obtained:

$$\mathbf{v}_i \mathbf{v}_i^T = \mathbf{u}_i \left(\mathbf{I} - \mathbf{C}_{k-1}^T (\mathbf{C}_{k-1} \mathbf{C}_{k-1}^T)^{-1} \mathbf{C}_{k-1} \right) \mathbf{u}_i^T, \quad (7)$$

and, therefore, the both algorithms are equivalent [7]. This is because $(\mathbf{I} - \mathbf{C}_{k-1}^T (\mathbf{C}_{k-1} \mathbf{C}_{k-1}^T)^{-1} \mathbf{C}_{k-1}) = \mathbf{P}_{\mathbf{C}_{k-1}}^\perp$ is the projection matrix to the orthogonal compliment space against the already selected sensor vector space, and therefore the absolute value of sensor-candidate matrix in the orthogonal compliment space $\mathbf{u}_i (\mathbf{I} - \mathbf{C}_{k-1}^T (\mathbf{C}_{k-1} \mathbf{C}_{k-1}^T)^{-1} \mathbf{C}_{k-1}) \mathbf{u}_i^T$ exactly corresponds to the absolute value of \mathbf{v}_i which is the sensor-candidate vector subtracted by the already selected sensor components in the k th step. See in Appendix for the detailed proof.

Although we derive an efficient way to recursively calculate $(\mathbf{C}_k \mathbf{C}_k^T)^{-1}$ used in the algorithm when the new sensor is found and the step number k is incremented, as follows:

$$\begin{aligned} (\mathbf{C}_k \mathbf{C}_k^T)^{-1} &= \left[\begin{array}{c} \mathbf{C}_{k-1} \\ \mathbf{u}_{i_k} \end{array} \right] \left[\begin{array}{cc} \mathbf{C}_{k-1}^T & \mathbf{u}_{i_k}^T \end{array} \right]^{-1} \\ &= \begin{pmatrix} \mathbf{A} & \mathbf{b}^T \\ \mathbf{b} & d \end{pmatrix}, \end{aligned} \quad (8)$$

where

$$\begin{aligned} \mathbf{A} &= (\mathbf{C}_{k-1} \mathbf{C}_{k-1}^T)^{-1} \\ &= \left\{ \mathbf{I} + \frac{\mathbf{C}_{k-1} \mathbf{u}_{i_k}^T \mathbf{u}_{i_k} \mathbf{C}_{k-1}^T (\mathbf{C}_{k-1} \mathbf{C}_{k-1}^T)^{-1}}{\mathbf{u}_{i_k} (\mathbf{I} - \mathbf{C}_{k-1}^T (\mathbf{C}_{k-1} \mathbf{C}_{k-1}^T)^{-1} \mathbf{C}_{k-1}) \mathbf{u}_{i_k}^T} \right\}, \\ \mathbf{b} &= \frac{-\mathbf{u}_{i_k} \mathbf{C}_{k-1}^T (\mathbf{C}_{k-1} \mathbf{C}_{k-1}^T)^{-1}}{\mathbf{u}_{i_k} (\mathbf{I} - \mathbf{C}_{k-1}^T (\mathbf{C}_{k-1} \mathbf{C}_{k-1}^T)^{-1} \mathbf{C}_{k-1}) \mathbf{u}_{i_k}^T}, \\ d &= \frac{1}{\mathbf{u}_{i_k} (\mathbf{I} - \mathbf{C}_{k-1}^T (\mathbf{C}_{k-1} \mathbf{C}_{k-1}^T)^{-1} \mathbf{C}_{k-1}) \mathbf{u}_{i_k}^T}, \end{aligned}$$

the total computational speed of the previous QR method is faster than that of the greedy algorithm and the previous QR method is generally chosen for this former part in the condition of $k < r$ except for the validation in the present paper. This algorithm is not straightforwardly used for the practical applications, but the algorithm is described in Alg. 3.

Algorithm 3 Determinant-based greedy algorithm for sparse sensor placement for $k \leq r$ (corresponds to the previous QR algorithm of $p = r$)

Set sensor-candidate matrix \mathbf{U} .

$$\mathbf{u}_i = [\mathbf{U}_{i,1} \mathbf{U}_{i,2} \dots \mathbf{U}_{i,r}]$$

$$i \leftarrow \arg \max_i (1 + \mathbf{u}_i \mathbf{u}_i^T)$$

$$H_{1,i} = 1$$

$$\mathbf{C} = \mathbf{u}_i$$

$$[\mathbf{U}_{i,1} \mathbf{U}_{i,2} \dots \mathbf{U}_{i,r}] \leftarrow [0, 0, \dots, 0]$$

for $k = 2, \dots, r$ **do**

$$\mathbf{u}_i = [\mathbf{U}_{i,1} \mathbf{U}_{i,2} \dots \mathbf{U}_{i,r}]$$

$$i \leftarrow \arg \max_i \mathbf{u}_i (\mathbf{I} - \mathbf{C}^T (\mathbf{C} \mathbf{C}^T)^{-1} \mathbf{C}) \mathbf{u}_i^T$$

Update $(\mathbf{C} \mathbf{C}^T)^{-1}$ using Eq. 8

$$H_{k,i} = 1$$

$$[\mathbf{U}_{i,1} \mathbf{U}_{i,2} \dots \mathbf{U}_{i,r}] \leftarrow [0, 0, \dots, 0]$$

end for

In case of $k \geq r$, the maximization of determinant of $\mathbf{C}^T \mathbf{C}$ is simply considered (see, e.g., [13] for detailed derivation.).

$$\begin{aligned} \det(\mathbf{C}_k^T \mathbf{C}_k) &= \det \left[\begin{array}{c} \mathbf{C}_{k-1}^T \mathbf{u}_i^T \\ \mathbf{u}_i \end{array} \right] \left[\begin{array}{c} \mathbf{C}_{k-1} \\ \mathbf{u}_i \end{array} \right] \\ &= (1 + \mathbf{u}_i (\mathbf{C}_{k-1}^T \mathbf{C}_{k-1})^{-1} \mathbf{u}_i^T) \det(\mathbf{C}_{k-1}^T \mathbf{C}_{k-1}). \end{aligned} \quad (9)$$

Therefore,

$$\begin{aligned} i &= \arg \max_i \det(\mathbf{C}_{k-1}^T \mathbf{C}_{k-1} + \mathbf{u}_i^T \mathbf{u}_i) \\ &= \arg \max_i (1 + \mathbf{u}_i (\mathbf{C}_{k-1}^T \mathbf{C}_{k-1})^{-1} \mathbf{u}_i^T). \end{aligned} \quad (10)$$

The complexity of this procedure is only $O(r^2)$ for one candidate sensor vector when inverse $(\mathbf{C}_{k-1}^T \mathbf{C}_{k-1})^{-1}$ is known, and the complexity when searching all components of vector becomes $O(nr^2)$. The inverse $(\mathbf{C}_k^T \mathbf{C}_k)^{-1}$ can be computed recursively using inverse matrix lemma when the new sensor is found and the the step number

k is incremented, as follows:

$$\begin{aligned}
& (\mathbf{C}_k^T \mathbf{C}_k)^{-1} \\
&= (\mathbf{C}_{k-1}^T \mathbf{C}_{k-1} + \mathbf{u}_i^T \mathbf{u}_i)^{-1} \\
&= (\mathbf{C}_{k-1}^T \mathbf{C}_{k-1})^{-1} \\
& \quad \left(\mathbf{I} - \mathbf{u}_i^T \left(1 + \mathbf{u}_i (\mathbf{C}_{k-1}^T \mathbf{C}_{k-1})^{-1} \mathbf{u}_i^T \right)^{-1} \mathbf{u}_i (\mathbf{C}_{k-1}^T \mathbf{C}_{k-1})^{-1} \right) \\
\end{aligned} \tag{11}$$

Algorithm 4 Determinant-based greedy algorithm for sparse sensor placement for $k > r$

Set sensor-candidate matrix \mathbf{U} .

Obtain \mathbf{H}_0 using the previous QR algorithm (or Alg. 3) for the number of the sensors $p_0 = r$.

Set $(\mathbf{C}^T \mathbf{C})^{-1} = (\mathbf{U}^T \mathbf{H}_0^T \mathbf{H}_0 \mathbf{U})^{-1}$

for i of sensor position chosen by conventional greedy algorithm **do**

Set $\mathbf{U}_i = [\mathbf{U}_{i,1} \mathbf{U}_{i,2} \dots \mathbf{U}_{i,r}] = [0, 0, \dots, 0]$

end for

for $k = p_0 + 1, \dots, p$ **do**

$\mathbf{U}_i = [\mathbf{U}_{i,1} \mathbf{U}_{i,2} \dots \mathbf{U}_{i,r}]$

$i \leftarrow \arg \max_i \left(1 + \mathbf{u}_i (\mathbf{C}^T \mathbf{C})^{-1} \mathbf{u}_i \right)$

$(\mathbf{C}^T \mathbf{C})^{-1} \leftarrow$

$(\mathbf{C}^T \mathbf{C})^{-1} \left(\mathbf{I} - \mathbf{u}_i^T \left(1 + \mathbf{u}_i (\mathbf{C}^T \mathbf{C})^{-1} \mathbf{u}_i^T \right)^{-1} \mathbf{u}_i (\mathbf{C}^T \mathbf{C})^{-1} \right)$

$H_{k,i} = 1$

$[\mathbf{U}_{i,1} \mathbf{U}_{i,2} \dots \mathbf{U}_{i,r}] \leftarrow [0, 0, \dots, 0]$

end for

C. Unified Expression for Proposed Algorithm

Here, we can introduce the unified expressions for both cases in which the number of the sensors is less than that of the modes and the number of the sensors is greater than or equal to that of the modes. In this case, the maximization of the term $\det(\mathbf{C}^T \mathbf{C} + \epsilon \mathbf{I})$, here ϵ is a sufficiently small number. This objective function is approximately corresponding to $\sim \det(\mathbf{C}^T \mathbf{C})$ when the number of sensor is greater than or equal to that of

the modes. On the other hand, when the number of the sensor p is less than that of the modes r , it becomes

$$\begin{aligned}
\det(\mathbf{C}^T \mathbf{C} + \epsilon \mathbf{I}) &= \epsilon^r \det \left(\mathbf{I} + \frac{1}{\epsilon} \mathbf{C}^T \mathbf{C} \right) \\
&= \epsilon^r \det \left(\mathbf{I} + \frac{1}{\epsilon} \mathbf{C} \mathbf{C}^T \right) \\
&= \epsilon^{r-p} \det(\mathbf{C} \mathbf{C}^T + \epsilon \mathbf{I}),
\end{aligned} \tag{12}$$

and then the objective function corresponds to the maximization of $\det(\mathbf{C} \mathbf{C}^T + \epsilon \mathbf{I}) \sim \det(\mathbf{C} \mathbf{C}^T)$ as we did in the previous subsection. Therefore, the approximated objective function is defined to be $\det(\mathbf{C}^T \mathbf{C} + \epsilon \mathbf{I})$ which asymptotically approaches to the maximization of determinant in the limit of ϵ goes to 0. Although this function should not be implemented in the computational code because it may includes large round-off error when ϵ is sufficiently small to neglect its effects, this approximated function will be used for the proof of submodularity and discussion of the approximation rate in the next session.

III. SUBMODULAR FUNCTIONAL AND APPROXIMATION RATE

The objective function $f(S) = \log \det(\mathbf{C}_S^T \mathbf{C}_S + \epsilon \mathbf{I})$ is proved to be the monotone submodular function and then the approximation rate of the greedy algorithm is discussed in this section, where S is defined to be the sensor set. The two sensor sets S and T are considered, and the set S is assumed to be a subset of T :

$$S \subset T \tag{13}$$

In this condition, the submodular function is defined as follows:

$$f(S \cup \{i\}) - f(S) \geq f(T \cup \{i\}) - f(T), \tag{14}$$

where i is an arbitrary element which satisfies $i \in T \setminus S$. $f(S) = \log \det(\mathbf{C}^T \mathbf{C} + \epsilon \mathbf{I})$ becomes submodular function.

$f(S) = \log \det(\mathbf{C}_S^T \mathbf{C}_S + \epsilon \mathbf{I})$ is a submodular function, where \mathbf{C}_S^T is a sensor matrix of set S .

Proof. The \mathbf{C} matrices of sensor sets S and T are denoted to be \mathbf{C}_S and \mathbf{C}_T , respectively.

$$\begin{aligned}
& f(S \cup \{i\}) - f(S) \\
&= \log \det(\mathbf{C}_S^T \mathbf{C}_S + \mathbf{u}_i^T \mathbf{u}_i + \epsilon \mathbf{I}) - \log \det(\mathbf{C}_S^T \mathbf{C}_S + \epsilon \mathbf{I}) \\
&= \log \det((\mathbf{C}_S^T \mathbf{C}_S + \mathbf{u}_i^T \mathbf{u}_i + \epsilon \mathbf{I})(\mathbf{C}_S^T \mathbf{C}_S + \epsilon \mathbf{I})^{-1}) \\
&= \log \det(\mathbf{I} + \mathbf{u}_i^T \mathbf{u}_i (\mathbf{C}_S^T \mathbf{C}_S + \epsilon \mathbf{I})^{-1}) \\
&= \log(1 + \mathbf{u}_i (\mathbf{C}_S^T \mathbf{C}_S + \epsilon \mathbf{I})^{-1} \mathbf{u}_i^T) \tag{15}
\end{aligned}$$

and

$$\begin{aligned}
& f(T \cup \{i\}) - f(T) \\
&= \log \det(1 + \mathbf{u}_i (\mathbf{C}_T^T \mathbf{C}_T + \epsilon \mathbf{I})^{-1} \mathbf{u}_i^T) \\
&= \log \det(1 + \mathbf{u}_i (\mathbf{C}_S^T \mathbf{C}_S + \mathbf{C}_{T \setminus S}^T \mathbf{C}_{T \setminus S} + \epsilon \mathbf{I})^{-1} \mathbf{u}_i^T) \\
&= \log \det(1 + \mathbf{u}_i (\mathbf{C}_S^T \mathbf{C}_S + \epsilon \mathbf{I})^{-1} \\
&\quad (\mathbf{I} - \mathbf{C}_{T \setminus S}^T (\mathbf{I} + \mathbf{C}_{T \setminus S} (\mathbf{C}_S^T \mathbf{C}_S + \epsilon \mathbf{I})^{-1} \mathbf{C}_{T \setminus S}^T)^{-1} \\
&\quad \mathbf{C}_{T \setminus S} (\mathbf{C}_S^T \mathbf{C}_S + \epsilon \mathbf{I})^{-1})) \\
&= \log \det(1 + \mathbf{u}_i (\mathbf{C}_S^T \mathbf{C}_S + \epsilon \mathbf{I})^{-1} \mathbf{u}_i^T \\
&\quad - \mathbf{u}_i (\mathbf{C}_S^T \mathbf{C}_S + \epsilon \mathbf{I})^{-1} \mathbf{C}_{T \setminus S}^T \\
&\quad (\mathbf{I} + \mathbf{C}_{T \setminus S} (\mathbf{C}_S^T \mathbf{C}_S + \epsilon \mathbf{I})^{-1} \mathbf{C}_{T \setminus S}^T)^{-1} \\
&\quad \mathbf{C}_{T \setminus S} (\mathbf{C}_S^T \mathbf{C}_S + \epsilon \mathbf{I})^{-1} \mathbf{u}_i^T) \tag{16}
\end{aligned}$$

The second terms in Eqs. 15 and 16 are always positive and the last term in the logarithm of Eq. 16 is always non-positive because the matrix inside between \mathbf{u}_i and \mathbf{u}_i^T is symmetric and the corresponding quadratic forms should be always positive and non-negative, respectively. Comparing terms inside the logarithm in Eqs. 15 and 16, we get

$$f(S \cup \{i\}) - f(S) \geq f(T \cup \{i\}) - f(T), \tag{17}$$

and f is a submodular function. \square

In addition to the submodularity, f is monotone.

Proof. Consider an arbitrary set S and an arbitrary element $i \in S \setminus V$. In this case,

$$\begin{aligned}
f(S \cup \{i\}) &= \log \det(\mathbf{C}_S^T \mathbf{C}_S + \mathbf{u}_i^T \mathbf{u}_i + \epsilon \mathbf{I}) \\
&= \log \det(\mathbf{C}_S^T \mathbf{C}_S + \epsilon \mathbf{I}) + \log \det(\mathbf{I} + \mathbf{u}_i^T \mathbf{u}_i (\mathbf{C}_S^T \mathbf{C}_S + \epsilon \mathbf{I})^{-1}) \\
&= f(S) + \log(1 + \mathbf{u}_i (\mathbf{C}_S^T \mathbf{C}_S + \epsilon \mathbf{I})^{-1} \mathbf{u}_i^T) \tag{18}
\end{aligned}$$

Here, $\log(1 + \mathbf{u}_i (\mathbf{C}_S^T \mathbf{C}_S + \epsilon \mathbf{I})^{-1} \mathbf{u}_i^T) > 0$ because the matrix of the quadratic form is symmetric and then it is nonnegative. Therefore,

$$f(S \cup \{i\}) > f(S) \tag{19}$$

and f is monotone submodular. \square

Therefore, the following inequality proved Nemhauser et al. can be applied to the monotone submodular function[14].

$$\left(1 - \left(1 - \frac{1}{k}\right)\right)^k f(S_{\text{opt}}) \leq f(S_{\text{greedy}}) \tag{20}$$

Here, k denotes the number of sensors, $S_{\text{opt}} \in V$ is an optimum solution, and $S_{\text{greedy}} \in V$ is the solution obtained by the greedy algorithm including the present formulation. Here, the factor $\alpha_k = \left(1 - \left(1 - \frac{1}{k}\right)\right)^k$ is monotonically decreasing and approaches to $1 - 1/e \sim 0.63$, when $k \rightarrow \infty$. Therefore,

$$0.63 f(S_{\text{opt}}) \leq f(S_{\text{greedy}}) \tag{21}$$

and this provides the lower bounds of the greedy approximation.

IV. RESULTS AND DISCUSSIONS

The numerical experiments are conducted and the proposed methods are validated. Hereinafter, three different implementations of the greedy methods are compared: QR, DG and QD methods listed in Table II. Here, the QR method is the greedy method proposed in the previous study[7], the DG method is the greedy method for the pure maximization of the determinant, and the QD method is the greedy method, the former part of which

is replaced by the QR method which is mathematically proved to be the equivalent algorithm to the the greedy method for the pure maximization of the determinant. Table III explains the computational complexities of each method for selecting p th sensors. The QD method is introduced because the QR implementation for the former greedy optimization is much faster than the DG method, and that both implementations are demonstrated to give us the same numerical optimized solution without being disturbed by round-off errors in the practical situations. In addition to greedy methods, a random selection and the convex approximation method[12] are evaluated for the reference.

TABLE II
GREEDY SENSOR SELECTION METHODS INVESTIGATED IN THE PRESENT STUDY

| Name | Method | Implementation |
|---|---|-----------------|
| QR[7] | $p \leq r$: QR for \mathbf{C} | Alg. 1 |
| | $p > r$: QR for $\mathbf{C}\mathbf{C}^T$ | Alg. 1 |
| DG (present) ^a | $p \leq r$: $\arg \max \det(\mathbf{C}\mathbf{C}^T)$ | Alg. 3 (Alg. 2) |
| | $p > r$: $\arg \max \det(\mathbf{C}^T\mathbf{C})$ | Alg. 4 (Alg. 2) |
| QD (present, recommended) ^a | $p \leq r$:QR for \mathbf{C} | Alg. 1 (Alg. 2) |
| | $p > r$: $\arg \max \det(\mathbf{C}^T\mathbf{C})$ | Alg. 4 (Alg. 2) |

^a DG and QD are mathematically equivalent algorithms as proved in the present paper.

TABLE III
COMPUTATIONAL COMPLEXITIES OF EACH METHOD FOR SELECTING p TH SENSORS.

| Name | Computational complexity |
|-------------|---|
| QR[7] | $p \leq r : O(pnr)$ |
| | $p > r : O(pn^2)$ |
| DG | $p \leq r : O(pnr^2)$ |
| | $p > r : O(pnr^2)$ |
| QD(present) | $p \leq r : O(pnr)$ |
| | $p > r : O(pnr^2)$ |
| convex[12] | $O(n^3)$ per iterations |
| | *usually converges around 200 iterations. |

A. Random sensor problem

The random sensor-candidate matrices, $\mathbf{U} \in \mathbb{R}^{1000 \times r}$, were set, where the component of the matrices is given by the Gaussian distribution of $\mathcal{N}(0, 1)$ in this validation. The random selection, the convex approximation method, QR, DG and QD listed in Table II are evaluated. After selecting sensors, the determinant of $\mathbf{C}\mathbf{C}^T = \mathbf{H}\mathbf{U}\mathbf{U}^T\mathbf{H}^T$ ($p \leq r$) and $\mathbf{C}^T\mathbf{C} = \mathbf{U}^T\mathbf{H}^T\mathbf{H}\mathbf{U}$ ($p > r$) are calculated using both sensor-candidate matrices. Figure 2 shows the relationship between the determinant of $\mathbf{C}\mathbf{C}^T$ ($p \leq r$) and $\mathbf{C}^T\mathbf{C}$ ($p > r$) and a number of sensors, p in POD mode $r = 10$ for the random sensor problem, obtained by the random selection (black solid line with close circle), the convex approximation method (blue solid line with close circle), QR (red solid line with close circle), DG (black dot line with open circle), and QD (gray solid line with close circle). All plots are normalized by the determinant of $\mathbf{C}\mathbf{C}^T$ ($p \leq r$) and $\mathbf{C}^T\mathbf{C}$ ($p > r$) of QR. In the case of $p \leq r$, the normalized determinant of $\mathbf{C}\mathbf{C}^T$ of DG and QD is the same as that of QR, and we can confirm what shown in the previous theoretical procedure. On the other hand, in the case of $p > r$, the normalized determinants of $\mathbf{C}^T\mathbf{C}$ of both DR and QD increase as the number of sensors increases. Although the computational cost or time of the convex approximation method is much bigger than that of other calculation methods, the convex approximation method obtains the normalized determinant of $\mathbf{C}^T\mathbf{C}$ in $p < 8$ and $p > 15$. Figure 3 shows the relationship the computational time and the number of sensors, p in POD mode $r = 10$ for the random sensor problem. Table III explains that the computational time of convex approximation algorithm is the longest in all calculation methods. The computational times of QR and QD in $p \leq r$ are the same as each other and gradually increases as the number of sensors increases.

However, the computational time of QR rapidly increases at $p = 11$ because the dimension of QR decomposition increases from $\mathbf{U} \in \mathbb{R}^{n \times r}$ to $\mathbf{U}\mathbf{U}^T \in \mathbb{R}^{n \times n}$. As opposed to QR, the trend of QD computational time keeps in $1 \leq p \leq 20$. Therefore, in the random sensor problem, QD proposed in this paper is more effective for sparse sensor placement than the convex algorithm because the determinant of $\mathbf{C}\mathbf{C}^T$ ($p \leq r$) and $\mathbf{C}^T\mathbf{C}$ ($p > r$) is larger and the calculation time is much shorter than that of other calculation methods in the case of $1 \leq p \leq 20$ (POD mode $r : 10$) for the random sensor problem.

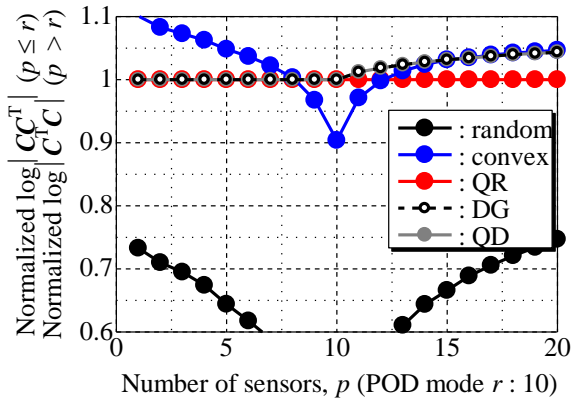


Fig. 2. Normalized by the determinant of $\mathbf{C}\mathbf{C}^T$ ($p \leq r$) and $\mathbf{C}^T\mathbf{C}$ ($p > r$) vs. number of sensors in POD modes $r = 10$ for random sensor problem

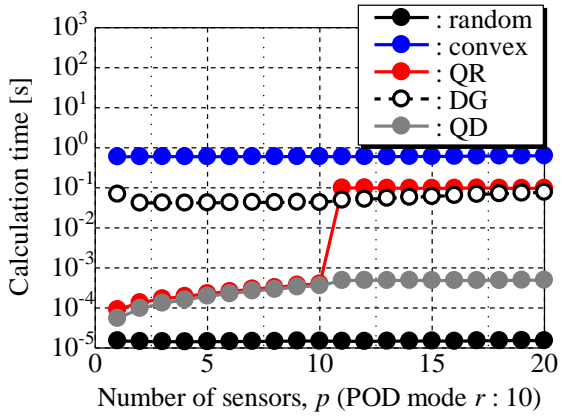


Fig. 3. Calculation time vs. number of sensors in POD modes $r = 10$ for random sensor problem

B. NOAA-SST

A data set that we adopt is the NOAA OISST (NOAA-SST) V2 mean sea surface temperature set, comprising weekly global sea surface temperature measurements in the years between 1990 and 2000[15]. There are a total of 520 snapshots on a 360×180 spatial grid (Fig. 4). Figure 5 shows the relationship between the estimation error and the number of POD modes, where the estimation error is defined to be the ratio of the difference between reconstructed data and the full observation data to the full observation. In the case of NOAA-SST, the POD modes are truncated and the $r = 10$ low-dimensional representation are obtained. Figure 5 shows the minimum estimation error is 0.30 in $r = 10$. We consider the results of the sensor selection problem (The number of sensors, $p : 1-20$) solved by each method; the random selection, the convex approximation method[12], QR[7], DG and QD listed in Table II. The NOAA-SST dataset truncated to the $r = 10$ POD modes is used in this study. Figure 6 shows sensor positions selected by the random selection, the convex approximation method, QR and QD, respectively in the case of $r = p = 10$. Note that all sensors of QD locate the same position as that of DG in all cases as well as in the previous random sensor problem.

Figure 7 shows the relationship between the estimation error and the number of sensors in POD mode $r = 10$ for NOAA-SST problem. All estimation errors decreases as the number of sensors increase. In the case of $p = 10$, three estimation error of QR, DG and QD coincides with each other because all sensor locations are the same as each other. After that ($p > r$), the estimation errors of both DG and QD are also the same as each other as well as in the random sensor problem. Although the estimation error of QR also decreases as the number of sensors increases, QR cannot select much better sensor

positions that DG and QD, which corresponds to the fact that it is not clear in $p > r$. Figure 8 shows the calculation time of each method for obtaining sensors in each condition. Although the trend in Fig. 8 is the same as that in Fig. 3, it is noticeable that the calculation time of the convex approximation method is approximately three hours, however, that of QD is just a few seconds with a lower estimation error as well as the computational time for the convex approximation method. According to these results, the proposing method, which called QD in this paper, is shown to be a more efficient method combining the best properties of shorter computational time and more high accuracy sensor selection entirely the number of sensors around that of the POD mode ($r = 10$).

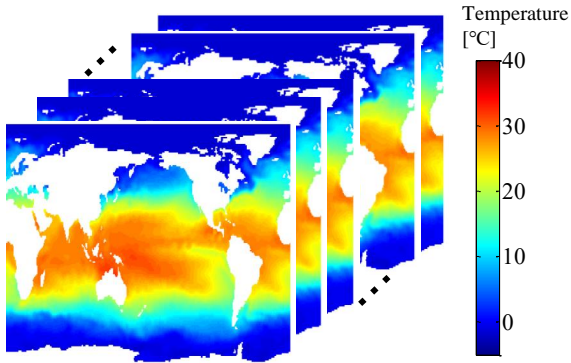


Fig. 4. Data set

V. CONCLUSIONS

The sparse sensor placement problem is considered for the least square estimation. First, the objective function of the problem is redefined to be the maximization of the determinant of the matrix appearing in pseudo inverse matrix operations, leading to the maximization of the corresponding confidence intervals. The procedure for the maximization of determinant of the corresponding matrix is proved to be the same as that of the previous QR method in the case of the number of sensors less

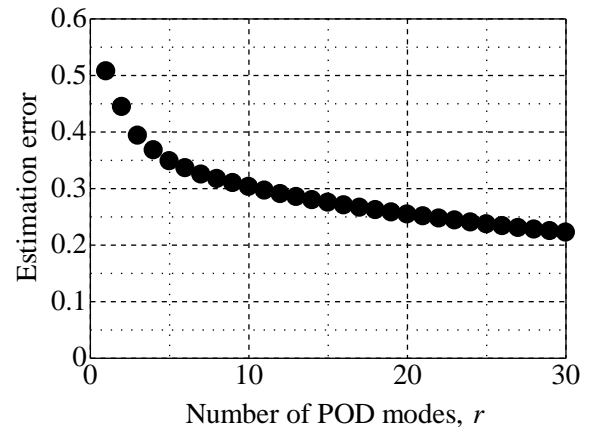


Fig. 5. Estimation error vs. number of POD modes for NOAA-SST problem

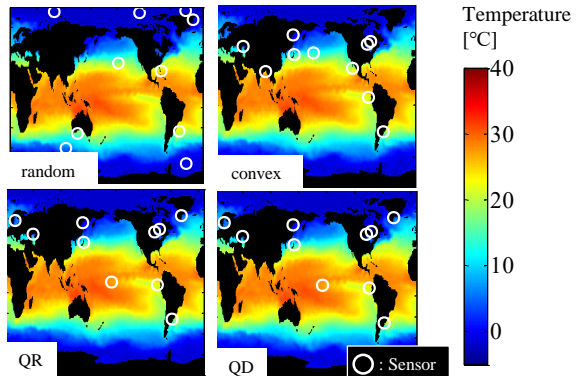


Fig. 6. Sensor position in $r = p = 10$ for NOAA-SST sensor problem

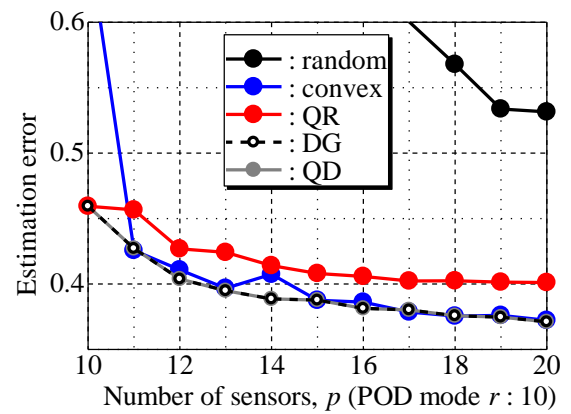


Fig. 7. Estimation error vs. the number of sensors in POD mode $r = 10$ for NOAA-SST problem

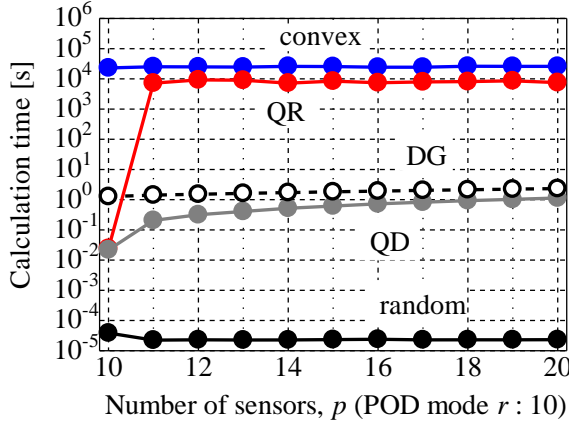


Fig. 8. Calculation time vs. the number of sensors in POD mode $r = 10$ for NOAA-SST problem

than that of state variables. On the other hand, the new algorithm in the case of the number of sensors greater than that of state variables is developed. The unified formulation is derived, and the lower bound of the objective function given by this algorithm is shown using the monotone submodularity. In a new algorithm, optimal sensors are obtained by QR method until the number of sensors is equal to state variables and, after that, new sensors are calculated by a proposed determinant-based greedy method which is accelerated by both determinant formula and matrix inversion lemma. The effectiveness of this algorithm on data-sets related to global climate dataset is demonstrated by comparing with the results by the other algorithms. The calculation time of the proposed extended determinant-based greedy algorithm is shown to be smaller than that of other methods with almost the minimum level of estimation errors. One weakness of the new algorithm is a robustness of noise. The algorithm does not work well for noisy dataset. The improvement of the greedy method will be the subject of challenging future research.

ACKNOWLEDGEMENTS

The second author T.N. is grateful for support of the grant JPMJPR1678 of JST Presto.

REFERENCES

- [1] G. Berkooz, P. Holmes, and L. J. Lumley, “The proper orthogonal decomposition in the analysis of turbulent flows,” *Annual Review of Fluid Mechanics*, vol. 25, no. 1971, pp. 539–575, 1993.
- [2] K. Taira, S. L. Brunton, S. T. Dawson, C. W. Rowley, T. Colonius, B. J. McKeon, O. T. Schmidt, S. Gordeyev, V. Theofanis, and L. S. Ukeiley, “Modal analysis of fluid flows: An overview,” *AIAA Journal*, pp. 4013–4041, 2017.
- [3] P. J. Schmid, “Dynamic mode decomposition of numerical and experimental data,” *Journal of Fluid Mechanics*, vol. 656, no. July 2010, pp. 5–28, 2010.
- [4] J. N. Kutz, S. L. Brunton, B. W. Brunton, and J. L. Proctor, *Dynamic mode decomposition: data-driven modeling of complex systems*. SIAM, 2016, vol. 149.
- [5] T. Nonomura, H. Shibata, and R. Takaki, “Dynamic mode decomposition using a kalman filter for parameter estimation,” *AIP Advances*, vol. 8, p. 105106, 2018.
- [6] ———, “Extended-kalman-filter-based dynamic mode decomposition for simultaneous system identification and denoising,” *PloS one*, vol. 14, p. e0209836, 2019.
- [7] K. Manohar, B. W. Brunton, J. N. Kutz, and S. L. Brunton, “Data-driven sparse sensor placement for reconstruction: Demonstrating the benefits of exploiting known patterns,” *IEEE Control Systems Magazine*, vol. 38, no. 3, pp. 63–86, June 2018.
- [8] S. Chaturantabut and D. C. Sorensen, “Nonlinear model reduction via discrete empirical interpolation,” *SIAM Journal on Scientific Computing*, vol. 32, no. 5, pp. 2737–2764, 2010.
- [9] Z. Drmac and S. Gugercin, “A new selection operator for the discrete empirical interpolation method—improved a priori error bound and extensions,” *SIAM Journal on Scientific Computing*, vol. 38, no. 2, pp. A631–A648, 2016.
- [10] K. Manohar, E. Kaiser, S. L. Brunton, and J. N. Kutz, “Optimized sampling for multiscale dynamics,” *Multiscale Modeling & Simulation*, vol. 17, no. 1, pp. 117–136, 2019.
- [11] S. Boyd and L. Vandenberghe, *Convex optimization*. Cambridge University Press, 2004.
- [12] S. Joshi and S. Boyd, “Sensor selection via convex optimization,” *IEEE Transactions on Signal Processing*, vol. 57, no. 2, pp. 451–462, 2009.
- [13] R. A. Horn and C. R. Johnson, *Matrix Analysis*, 2nd ed. New York, NY, USA: Cambridge University Press, 2012.

[14] G. L. Nemhauser, L. A. Wolsey, and M. L. Fisher, “An analysis of approximations for maximizing submodular set functions,” *Mathematical programming*, vol. 14, no. 1, pp. 265–294, 1978.

[15] NOAA/OAR/ESRL, “Noaa optimal interpolation (oi) sea surface temperature (sst) v2,” Boulder CO, July 2019. [Online]. Available: <https://www.esrl.noaa.gov/psd/>

APPENDIX

A. Equivalence for operations of QR and the present method in the case of $k \leq r$

Proof. (By Mathematical Induction.) We consider that

$$\mathbf{v}_i \mathbf{v}_i^T = \mathbf{u}_i \left(\mathbf{I} - \mathbf{C}_{n-1}^T \left(\mathbf{C}_{n-1} \mathbf{C}_{n-1}^T \right)^{-1} \mathbf{C}_{n-1} \right) \mathbf{u}_i^T. \quad (22)$$

Here, \mathbf{v}_i is expressed by \mathbf{u}_i :

$$\mathbf{v}_i = \mathbf{u}_i \mathbf{P}_k^{\text{QR}}, \quad (23)$$

where \mathbf{P}_k^{QR} is the projection matrix corresponding to the Gram-Schmidt operator used in Alg. 1. The squared norm of \mathbf{v}_i of the left-hand side Eq. 25 can be expressed:

$$\mathbf{v}_i \mathbf{v}_i^T = \mathbf{u}_i \mathbf{P}_k^{\text{QR}} \mathbf{u}_i^T. \quad (24)$$

On the other hand, the right-hand side of Eq. 25 can be expressed:

$$\mathbf{u}_i \left(\mathbf{I} - \mathbf{C}_{n-1}^T \left(\mathbf{C}_{n-1} \mathbf{C}_{n-1}^T \right)^{-1} \mathbf{C}_{n-1} \right) \mathbf{u}_i^T = \mathbf{u}_i \mathbf{P}_k^{\perp} \mathbf{u}_i^T. \quad (25)$$

where $\mathbf{P}_k^{\perp} = \left(\mathbf{I} - \mathbf{C}_{n-1}^T \left(\mathbf{C}_{n-1} \mathbf{C}_{n-1}^T \right)^{-1} \mathbf{C}_{n-1} \right)$.

Now, we will prove the following equation

$$\mathbf{P}_k^{\text{QR}} = \mathbf{P}_k^{\perp}, \quad (26)$$

and the equivalence for operations of the QR and present methods in the case of $k \leq r$ expressed in Eq. 22.

If $k = 1$, the equations are written as:

$$\mathbf{P}_1 = \mathbf{P}_1^{\text{QR}} = \mathbf{P}_1^{\perp} \quad (27)$$

because both algorithms select the first sensor based on maximizing the norm of the corresponding row vector of \mathbf{U} . If $k = 2$, the equations are expressed as:

$$\mathbf{P}_2^{\text{QR}} = \mathbf{I} - \frac{\mathbf{w}_1^T \mathbf{w}_1}{\|\mathbf{w}_1\|_2^2} \quad (28)$$

and

$$\begin{aligned} \mathbf{P}_2^{\perp} &= \mathbf{I} - \mathbf{C}_1^T \left(\mathbf{C}_1 \mathbf{C}_1^T \right)^{-1} \mathbf{C}_1 \\ &= \mathbf{I} - \mathbf{w}_1^T \left(\mathbf{w}_1 \mathbf{w}_1^T \right)^{-1} \mathbf{w}_1 \\ &= \mathbf{I} - \frac{\mathbf{w}_1^T \mathbf{w}_1}{\|\mathbf{w}_1\|_2^2}. \end{aligned} \quad (29)$$

Therefore, $\mathbf{P}_2^{\text{QR}} = \mathbf{P}_2^{\text{DG}}$ in Eqs. 28 and 29.

Now, we assume that

$$\mathbf{P}_n = \mathbf{P}_n^{\text{QR}} = \mathbf{P}_n^{\perp}. \quad (30)$$

If $k = n + 1$, the equations are expressed as:

$$\begin{aligned} \mathbf{P}_{n+1}^{\text{QR}} &= \\ &\left(\mathbf{I} - \frac{\mathbf{w}_1^T \mathbf{w}_1}{\|\mathbf{w}_1\|_2^2} \right) \left(\mathbf{I} - \frac{\mathbf{w}_2^T \mathbf{w}_2}{\|\mathbf{w}_2\|_2^2} \right) \cdots \left(\mathbf{I} - \frac{\mathbf{w}_{n-1}^T \mathbf{w}_{n-1}}{\|\mathbf{w}_{n-1}\|_2^2} \right) \left(\mathbf{I} - \frac{\mathbf{w}_n^T \mathbf{w}_n}{\|\mathbf{w}_n\|_2^2} \right) \\ &= \mathbf{P}_n^{\text{QR}} \left(\mathbf{I} - \frac{\mathbf{w}_n^T \mathbf{w}_n}{\|\mathbf{w}_n\|_2^2} \right) \\ &= \mathbf{P}_n \left(\mathbf{I} - \frac{\mathbf{w}_n^T \mathbf{w}_n}{\|\mathbf{w}_n\|_2^2} \right) \end{aligned} \quad (31)$$

$$\begin{aligned} \mathbf{P}_{n+1}^{\perp} &= \mathbf{I} - \mathbf{C}_n^T \left(\mathbf{C}_n \mathbf{C}_n^T \right)^{-1} \mathbf{C}_n \\ &= \mathbf{I} - \left(\begin{array}{cc} \mathbf{C}_{n-1}^T & \mathbf{u}_i^T \end{array} \right) \left(\mathbf{C}_n \mathbf{C}_n^T \right)^{-1} \left(\begin{array}{c} \mathbf{C}_{n-1}^T \\ \mathbf{u}_i^T \end{array} \right) \\ &= \left(\mathbf{I} - \mathbf{C}_{n-1}^T \left(\mathbf{C}_{n-1} \mathbf{C}_{n-1}^T \right)^{-1} \mathbf{C}_{n-1} \right) \left(\mathbf{I} - \frac{\mathbf{P}_n^T \mathbf{u}_i^T \mathbf{u}_i \mathbf{P}_n}{\mathbf{u}_i \mathbf{P}_n \mathbf{P}_n^T \mathbf{u}_i^T} \right) \\ &= \mathbf{P}_n \left(\mathbf{I} - \frac{\mathbf{P}_n^T \mathbf{u}_i^T \mathbf{u}_i \mathbf{P}_n}{\mathbf{u}_i \mathbf{P}_n \mathbf{P}_n^T \mathbf{u}_i^T} \right) \end{aligned} \quad (32)$$

See in Appendix B for detailed derivation. Here,

$$\mathbf{w}_n = \mathbf{u}_i \mathbf{P}_n \quad (33)$$

$$\mathbf{P}_{n+1}^{\perp} = \mathbf{P}_n \left(\mathbf{I} - \frac{\mathbf{w}_n^T \mathbf{w}_n}{\|\mathbf{w}_n\|_2^2} \right) \quad (34)$$

Assuming n th sensors selected up to $k = n$ are the same, the projection matrices for selecting the $(n + 1)$ th sensor are equal to each other, and the row norms calculated at $k = n + 1$ are the same each other from Eqs. 31 and 31.

Therefore, the equivalence of operations of QR and DG is proved in the case of the number of sensors: $1 \leq k \leq r$. \square

B. Derivation of \mathbf{P}_{n+1}^{QR}

$$\begin{aligned}
\mathbf{P}_{n+1}^{\perp} &= \mathbf{I} - \mathbf{C}_n^T \left(\mathbf{C}_n \mathbf{C}_n^T \right)^{-1} \mathbf{C}_k \\
&= \mathbf{I} - \left[\begin{array}{cc} \mathbf{C}_{n-1}^T & \mathbf{u}_i^T \end{array} \right] \left[\begin{array}{cc} \left(\mathbf{C}_{n-1} \mathbf{C}_{n-1}^T \right)^{-1} & \mathbf{0} \\ \mathbf{0} & \mathbf{0} \end{array} \right] \left[\begin{array}{c} \mathbf{C}_{n-1} \\ \mathbf{u}_i \end{array} \right] - \\
&= \frac{1}{\mathbf{u}_i^T \mathbf{P}_n \mathbf{u}_i} \left[\begin{array}{cc} \mathbf{C}_{n-1}^T & \mathbf{u}_i^T \end{array} \right] \left[\begin{array}{cc} \left(\mathbf{C}_{n-1} \mathbf{C}_{n-1}^T \right)^{-1} \mathbf{C}_{n-1} \mathbf{u}_i^T \mathbf{u}_i \mathbf{C}_{n-1}^T \left(\mathbf{C}_{n-1} \mathbf{C}_{n-1}^T \right)^{-1} & -\left(\mathbf{C}_{n-1} \mathbf{C}_{n-1}^T \right)^{-1} \mathbf{C}_{n-1} \mathbf{u}_i^T \\ -\mathbf{u}_i^T \mathbf{C}_{n-1}^T \left(\mathbf{C}_{n-1} \mathbf{C}_{n-1}^T \right)^{-1} & 1 \end{array} \right] \left[\begin{array}{c} \mathbf{C}_{n-1} \\ \mathbf{u}_i \end{array} \right] \\
&= \mathbf{I} - \mathbf{C}_{n-1}^T \left(\mathbf{C}_{n-1} \mathbf{C}_{n-1}^T \right)^{-1} \mathbf{C}_{n-1} \\
&\quad - \frac{1}{\mathbf{u}_i^T \mathbf{P}_n \mathbf{u}_i} \left(\mathbf{C}_{n-1}^T \left(\mathbf{C}_{n-1} \mathbf{C}_{n-1}^T \right)^{-1} \mathbf{C}_{n-1} \mathbf{u}_i^T \mathbf{u}_i \mathbf{C}_{n-1}^T \left(\mathbf{C}_{n-1} \mathbf{C}_{n-1}^T \right)^{-1} \mathbf{C}_{n-1} - \mathbf{C}_{n-1}^T \left(\mathbf{C}_{n-1} \mathbf{C}_{n-1}^T \right)^{-1} \mathbf{C}_{n-1} \mathbf{u}_i^T \mathbf{u}_i - \mathbf{u}_i^T \mathbf{u}_i \mathbf{C}_{n-1}^T \left(\mathbf{C}_{n-1} \mathbf{C}_{n-1}^T \right)^{-1} \mathbf{C}_{n-1} + \mathbf{u}_i^T \mathbf{u}_i \right) \\
&= \frac{\mathbf{I} - \mathbf{C}_{n-1}^T \left(\mathbf{C}_{n-1} \mathbf{C}_{n-1}^T \right)^{-1} \mathbf{C}_{n-1}}{\mathbf{u}_i^T \mathbf{P}_n \mathbf{u}_i} \left(\mathbf{u}_i^T \mathbf{u}_i \left(\mathbf{I} - \left(\mathbf{C}_{n-1}^T \left(\mathbf{C}_{n-1} \mathbf{C}_{n-1}^T \right)^{-1} \mathbf{C}_{n-1} \right) \right) \right) \\
&= \mathbf{P}_n - \frac{\mathbf{P}_n}{\mathbf{u}_i^T \mathbf{P}_n \mathbf{u}_i} \left(\mathbf{u}_i^T \mathbf{u}_i \mathbf{P}_n \right) \\
&= \mathbf{P}_n \left(\mathbf{I} - \frac{\mathbf{u}_i^T \mathbf{u}_i \mathbf{P}_n}{\mathbf{u}_i^T \mathbf{P}_n \mathbf{u}_i^T} \right) \\
&= \mathbf{P}_n \left(\mathbf{I} - \frac{\mathbf{P}_n \mathbf{u}_i^T \mathbf{u}_i \mathbf{P}_n}{\mathbf{u}_i^T \mathbf{P}_n \mathbf{u}_i^T} \right) \tag{35}
\end{aligned}$$